Memorias del XVI Congreso Latinoamericano de Control Automático, CLCA 2014
Octubre 14-17, 2014. Cancún, Quintana Roo, México

Tyre-road friction coefficient estimation based on tyre lateral deflection

C. Acosta Lua [*] **B. Castillo-Toledo, R. Cespi** [**]
S. Di Gennaro [***]

[*] *Departamento de Ciencias Tecnológicas, Universidad de Guadalajara, Ocotlán, México, (e-mail: cuauhtemoc.acosta@cuci.udg.mx)*
[**] *Centro de Investigación y de Estudios Avanzados, Guadalajara, México (e-mail: toledo@gdl.cinvestav.mx, riccardocespi@yahoo.it)*
[***] *Department of Information Engineering, Universita degli Studi de L'Aquila, L'Aquila, Italy (e-mail: stefano.digennaro@univaq.it)*

Abstract: In this paper we present the tyre-road friction coefficient estimation which depends on the estimation of tyre slip angle, lateral and vertical tyre forces, and the use of a brush model. The lateral force acting on the tyre is obtained by using the coefficient of a parabolic function which approximates the deflection profile inside the contact patch. The slip angle is estimated by a nonlinear observer for the vehicle longitudinal and lateral velocity and roll position and velocity. This technique is based on measurements of the yaw rate and steering angle, longitudinal and lateral acceleration usually available in modern vehicles. Effectiveness and performance of the proposed nonlinear observer and tyre-road friction coefficient estimation are shown making use of an accurate vehicle simulator for a maneuver made on different road surface conditions.

Keywords: Tyres, Four-wheel, Friction, Observers, Nonlinear models.

1. INTRODUCTION

Tyre-road friction force plays a key role in maintaining the stability and the controllability of vehicle dynamic motion. The estimation of the tyre-road friction coefficient is of fundamental importance in every active control systems. Active control can ensure a better performance of a vehicle, adding further actions to increase the driveability and safety, important especially in critical situations. The control action is usually determined on the basis of approximated models, simple enough to obtain an implementable controller, but accurate enough to capture the main aspects of the physics of the problem. Lateral and yaw dynamics are the usual dynamics considered in the control synthesis, while the other dynamics are assumed to be bounded perturbations. For example, the roll dynamics are usually neglected. However, in some cases, such as that of tall vehicles with no active devices on the suspensions, the assumption that these perturbative dynamics have a limited influence is not verified, and should be taken into account in the control design. Another problem considered in this work is the fact that some of the state variables, necessary to implement such control strategies, are usually not measured, due to sensor cost and space occupancy in the vehicle. For instance, the lateral velocity is rarely measured. Therefore, in order to obtain a satisfactory control performance, these state variables have to be determined from other measurements, such as longitudinal and lateral acceleration, longitudinal velocity, yaw rate and steer angle. For, an observer for the lateral velocity and roll position and velocity is designed to reconstruct the unmeasured variables. Earlier works on observers, limited to the estimation of the lateral velocity, are mainly based on linear techniques as in (Farrelly and Wellstead, 1996) (Fukada, 1999) or quasilinear techniques as in (Peng *et al.*, 2004) (Venhovens and Naab, 1999). A nonlinear observer linearizing the error dynamics is proposed in (Kiencke and Daiss, 1997) (Kiencke and Nielsen, 2000). A similar observer is presented in (Hiemer *et al.*, 2005); containing an additional term forcing the dynamics of the nonlinear estimation error to those of a linear reference system. Linear and nonlinear observers using the sliding mode techniques are proposed in (Baffet *et al.*, 2007) (Stephant *et al.*, 2007). Other proposed observers are based on the extended Kalman filter (Ray, 1995) (Suissa *et al.*, 1996) (Best *et al.*, 2000). On the other hand, the tyre-road friction coefficient is critical to vehicle longitudinal, lateral and roll dynamics and control because tyre is the only contact part between the vehicle body and the road. However, direct measurement of tyre-road friction coefficient is impossible in practice. This paper presents a technic based on tyre carcass deflection and observer estimations using a tyre brush model. Some similar approach based on tyre optical sensors are presented in (Tuononen *et al.*, 2008) (Tuononen *et al.*, 2008) where the tyre deflection is used for tyre lateral force estimation and in (Tuononen, 2009) (Tuononen and Matilainen, 2009) (Tuononen, 2009) where the tyre deflection is used for aquaplaning detection. The paper is organized as follows. In Section 2, the mathematical model of a four wheels vehicle motion with roll dynamics is reviewed. In Section 3, the observer design is carried out. In Section 4 the tyre-road friction coefficient estimation is presented. In Section 5 some simulation results are given. Finally, some comments conclude the paper.

2. THE ACTIVE CONTROL PROBLEM FOR A GROUND VEHICLE

The dynamics of a ground vehicle can be described by the so–called Four Wheel Vehicle Motion model (FWVM) (Heydinger *et al.*, 1990) (Doumiati *et al.*, 2011)

$$\begin{aligned} m(\dot{v}_x - v_y\omega_z) &= ma_x - m_s h\omega_z\dot{\alpha}_x \\ m(\dot{v}_y + v_x\omega_z) &= ma_y + m_s h\ddot{\alpha}_x \\ J_z\dot{\omega}_z &= \mu_y(F_{y,f}l_f - F_{y,r}l_r) + J_{zx}\ddot{\alpha}_x \end{aligned} \tag{1}$$

where m, J_z are the total vehicle mass and inertia with respect to the perpendicular axis, l_f, l_r are the distances from the vehicle center of gravity ($C.G.$) to the front and rear tyres, a_x, a_y are the longitudinal and lateral accelerations, v_x, v_y are the longitudinal and lateral velocities of the $C.G.$, ω_z is the yaw rate, α_x is the roll angle, m_s is the so–called sprung mass, h is the distance between the center of gravity and the roll axis, and J_{xz} is the inertia product with respect to the longitudinal and yaw axes with δ the steering wheel angle(see Figure 1).

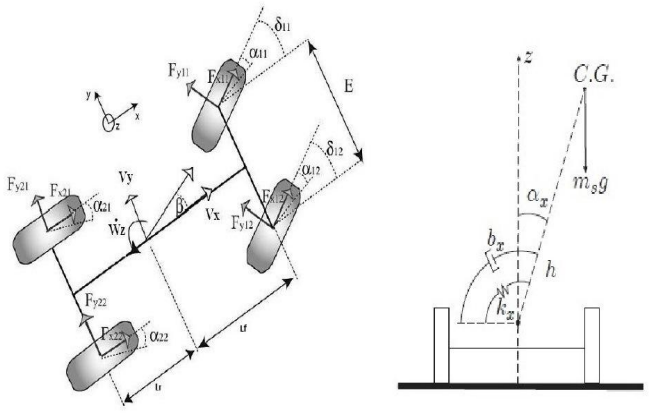

Fig. 1. Four Wheels Vehicle Model with Roll Dynamic

In (1), the vehicle roll acceleration can be expressed as follows (Mammar, 1999)**?** (Pacejka, 2005)

$$\begin{aligned} J_x\ddot{\alpha}_x = &-b_x\dot{\alpha}_x - k_x\alpha_x + m_s gh\sin\alpha_x \\ &+ m_s h(\dot{v}_y + \omega_z v_x)\cos\alpha_x + J_{xz}\dot{\omega}_z \end{aligned} \tag{2}$$

where $J_x = J_x^G + m_s h^2$ is the vehicle moment of inertia with respect to the longitudinal axis, J_x^G is the vehicle moment of inertia with respect to the longitudinal axis passing for the $C.G.$, g is the weight acceleration, and b_x, k_x are the suspension roll damping and stiffness(see Figure 1).

Considering small angles α_x, and considering that $J_{xz} \simeq 0$, from (1) and (2), we obtain the system dynamics

$$\begin{aligned} \dot{v}_x &= v_y\omega_z + a_x - \frac{m_s}{m}h\omega_z\omega_x \\ \dot{v}_y &= -v_x\omega_z + \frac{J_x}{J_{x,e}}a_y - \frac{k_{x,e}}{J_{x,s}}\alpha_x - \frac{b_x}{J_{x,s}}\omega_x \\ \dot{\omega}_z &= \frac{\mu_y}{J_z}(F_{y,f}l_f - F_{y,r}l_r) + \frac{1}{J_z}M_z \\ \dot{\alpha}_x &= \omega_x \\ \dot{\omega}_x &= -\frac{k_{x,e}}{J_{x,e}}\alpha_x - \frac{b_x}{J_{x,e}}\omega_x + \frac{m_s}{J_{x,e}}ha_y \end{aligned} \tag{3}$$

with

$$J_{x,e} = J_x - \frac{m_s^2}{m}h^2, \quad J_{x,s} = \frac{mJ_{x,e}}{m_s h}, \quad k_{x,e} = k_x - m_s gh.$$

Moreover, $F_{y,f}$, $F_{y,r}$ are the lateral forces of the front and rear axes, which are defined as the following (Doumiati *et al.*, 2011):

$$\begin{aligned} F_{y,f} &= F_{y,11}\cos\delta + F_{y,12}\cos\delta + F_{x,1}\sin\delta \\ F_{y,r} &= F_{y,21} + F_{y,22} \end{aligned} \tag{4}$$

with $F_{x,1}$, the front axle longitudinal force.
The tyre slip angles are defined according to the (FWVM) model (Doumiati *et al.*, 2011):

$$\begin{aligned} \alpha_{11} &= \delta - \arctan\left[\frac{v_x\beta + l_f\omega_z}{v_x - E\omega_z/2}\right] \\ \alpha_{12} &= \delta - \arctan\left[\frac{v_x\beta + l_f\omega_z}{v_x + E\omega_z/2}\right] \\ \alpha_{21} &= -\arctan\left[\frac{v_x\beta - l_f\omega_z}{v_x - E\omega_z/2}\right] \\ \alpha_{22} &= -\arctan\left[\frac{v_x\beta - l_f\omega_z}{v_x + E\omega_z/2}\right] \end{aligned} \tag{5}$$

where $\beta = v_x/v_y$ is the vehicle body sideslip angle.

This model describes the vehicle dynamics under the following assumptions

1. Pitch dynamic is neglected.
2. The system is rigid.
3. The suspension is passive.
4. The steering wheel angle $\delta_{11} = \delta_{12} = \delta$.
5. The front and rear track widhs (E) are assumed to be equal.
6. Camber angle is null.

Note that the longitudinal and lateral accelerations a_x, a_y in (3), which can be expressed in terms of the front/rear longitudinal and lateral tyre forces

$$\begin{aligned} a_x &= \frac{\mu_x}{m}\Big(-F_{y,11}\sin\delta - F_{y,12}\sin\delta + F_{x,1}\cos\delta\Big) \\ a_y &= \frac{\mu_y}{m}\Big(F_{y,11}\cos\delta + F_{y,12}\cos\delta + (F_{y,21} + F_{y,22}) \\ &\quad + F_{x,1}\sin\delta\Big) \end{aligned} \tag{6}$$

are measured by accelerometers, usually present aboard of a modern automobile. Here, μ_x is the longitudinal tyre-road friction coefficient.

3. OBSERVER DESIGN

In the following it is supposed that a_x, a_y, ω_z, v_x are measurable. This is an acceptable hypothesis in modern vehicles, usually equipped with the necessary sensors. The proposed nonlinear observer relies on a copy of the plant (3)

$$
\begin{aligned}
\dot{\hat{v}}_x &= \hat{v}_y\omega_z + a_x - \frac{m_s}{m}h\omega_z\hat{\omega}_x + k_{o1}(v_x - \hat{v}_x)\\
\dot{\hat{v}}_y &= -\hat{v}_x\omega_z + \frac{J_x}{J_{x,e}}a_y - \frac{k_{x,e}}{J_{x,s}}\hat{\alpha}_x - \frac{b_x}{J_{x,s}}\hat{\omega}_x\\
&\quad + (k_{o2} - \omega_z)(v_x - \hat{v}_x)\\
\dot{\hat{\alpha}}_x &= \hat{\omega}_x + k_{o3}(v_x - \hat{v}_x)\\
\dot{\hat{\omega}}_x &= -\frac{k_{x,e}}{J_{x,e}}\hat{\alpha}_x - \frac{b_x}{J_{x,e}}\hat{\omega}_x + \frac{m_s}{J_{x,e}}ha_y + k_{o4}(v_x - \hat{v}_x)
\end{aligned}
\tag{7}
$$

where $k_{o1}, \cdots, k_{o4}$ are the observer gains, to be determined. Using (3), (7), the dynamics of the estimation errors

$$
\begin{aligned}
e_{v_x} &= v_x - \hat{v}_x\\
e_{v_y} &= v_y - \hat{v}_y\\
e_{\alpha_x} &= \alpha_x - \hat{\alpha}_x\\
e_{\omega_x} &= \omega_x - \hat{\omega}_x
\end{aligned}
\tag{8}
$$

can be easily calculated

$$
\begin{aligned}
\dot{e}_{v_x} &= -k_{o1}e_{v_x} + \omega_z e_{v_y} - \frac{m_s}{m}h\omega_z e_{\omega_x}\\
\dot{e}_{v_y} &= -k_{o2}e_{v_x} - \frac{1}{J_{x,s}}(k_{x,e}e_{\alpha_x} + b_x e_{\omega_x})\\
\dot{e}_{\alpha_x} &= -k_{o3}e_{v_x} + e_{\omega_x}\\
\dot{e}_{\omega_x} &= -k_{o4}e_{v_x} - \frac{1}{J_{x,e}}(k_{x,e}e_{\alpha_x} + b_x e_{\omega_x})
\end{aligned}
\tag{9}
$$

where $J_{x,s} = m_e J_x/(m_s h)$. Equations (9) are linear and time varying due to the term ω_z. In the following it will be shown how to determine the gains $k_{o1}, \cdots, k_{o4}$ in (7) so that the exponential convergence of the estimation errors is ensured, under the following.

Assumption 1. The yaw angular velocity ω_z remains bounded for all $t \geq t_0$, i.e. $|\omega_z| \leq \omega_{z,\max}$. ◇

This assumption is physically reasonable, since the vehicle is finite energy system, the maximal yaw angular velocity remains bounded. In what follows, we derive an observer that, for $|\omega_z| > 0$ and under Assumption 1, will ensure the exponential convergence to zero of the estimation errors. Note that during a maneuver ω_z may pass through zero, but cannot be identically zero in a finite interval of time unless when the lateral forces are zero, namely when the vehicle is proceeding straight.

The design of the observer gains $k_{o1}, \cdots, k_{o4}$ in (7) is done using the following Lyapunov candidate

$$
\begin{aligned}
V_o(t,e) &= V_{o,1}(t, e_{v_x}, e_{v_y}) + V_{o,2}(e_{\alpha_x}, e_{\omega_x})\\
V_{o,1}(t,e) &= \frac{1}{2}(\gamma_1 e_{v_x}^2 + e_{v_y}^2) - \kappa_1 \mathcal{S}_{\omega_z} e_{v_x} e_{v_y}\\
V_{o,2}(e_{\alpha_x}, e_{\omega_x}) &= \frac{1}{2}\begin{pmatrix} e_{\alpha_x} \\ e_{\omega_x}\end{pmatrix}^T P_2 \begin{pmatrix} e_{\alpha_x} \\ e_{\omega_x}\end{pmatrix}
\end{aligned}
$$

with $e = \begin{pmatrix} e_{v_x}, e_{v_y}, e_{\alpha_x}, e_{\omega_x}\end{pmatrix}^T$, $\gamma_1 > \kappa_1^2 > 0$, $\kappa_1 \neq 0$ constant, $P_2 = P_2^T > 0$, and $\mathcal{S}_{\omega_z} = \text{sign}(\omega_z)$ the classical sign function

$$
\mathcal{S}_{\omega_z} = \begin{cases} 1 & \text{if } \omega_z > 0\\ 0 & \text{if } \omega_z = 0\\ -1 & \text{if } \omega_z < 0.\end{cases}
$$

To this aim, deriving the Lyapunov candidate along the dynamics (9), one works out

$$
\begin{aligned}
\dot{V}_o(t,e) &= \gamma_1 e_{v_x}\Big(- k_{o1}e_{v_x} + \omega_z e_{v_y} - \frac{m_s}{m}h\omega_z e_{\omega_x}\Big)\\
&\quad + e_{v_y}\Big(- k_{o2}e_{v_x} - \frac{k_{x,e}}{J_{x,s}}e_{\alpha_x} - \frac{b_x}{J_{x,s}}e_{\omega_x}\Big)\\
&\quad - \kappa_1 \mathcal{S}_{\omega_z} e_{v_x}\Big(- k_{o2}e_{v_x} - \frac{k_{x,e}}{J_{x,s}}e_{\alpha_x} - \frac{b_x}{J_{x,s}}e_{\omega_x}\Big)\\
&\quad - \kappa_1 \mathcal{S}_{\omega_z} e_{v_y}\Big(- k_{o1}e_{v_x} + \omega_z e_{v_y} - \frac{m_s}{m}h\omega_z e_{\omega_x}\Big)\\
&\quad - 2\kappa_1 \delta_{_D}(\omega_z)\dot{\omega}_z e_{v_x} e_{v_y}\\
&\quad + \begin{pmatrix} e_{\alpha_x} \\ e_{\omega_x}\end{pmatrix}^T P_2 A_2 \begin{pmatrix} e_{\alpha_x} \\ e_{\omega_x}\end{pmatrix} - \begin{pmatrix} e_{\alpha_x} \\ e_{\omega_x}\end{pmatrix}^T P_2 \begin{pmatrix} k_{o3} \\ k_{o4}\end{pmatrix} e_{v_x}
\end{aligned}
$$

where the derivative of $\mathcal{S}_{\omega_z}$ is given by

$$
\frac{d}{dt}\mathcal{S}_{\omega_z} = 2\delta_{_D}(\omega_z)\dot{\omega}_z
$$

with $\delta_{_D}(\omega_z)$ the Dirac distribution, and

$$
A_2 = \begin{pmatrix} 0 & 1 \\ -\frac{k_{x,e}}{J_{x,e}} & -\frac{b_x}{J_{x,e}}\end{pmatrix}.
$$

For $|\omega_z| > 0$ and under Assumption 1, $\delta_{_D}(\omega_z) = 0$ and

$$
\begin{aligned}
\dot{V}_o(t,e) &= -\Big(k_{o1}\gamma_1 - \kappa_1 k_{o2}\mathcal{S}_{\omega_z}\Big)e_{v_x}^2 - \kappa_1|\omega_z|e_{v_y}^2\\
&\quad - \left\| \begin{matrix} e_{\alpha_x} \\ e_{\omega_x}\end{matrix} \right\|_{Q_2}^2 + \Big(\gamma_1\omega_z - k_{o2} + \kappa_1 k_{o1}\mathcal{S}_{\omega_z}\Big)e_{v_x}e_{v_y}\\
&\quad + \Big(\kappa_1\frac{k_{x,e}}{J_{x,s}}\mathcal{S}_{\omega_z} - p_{21}k_{o3} - p_{22}k_{o4}\Big)e_{v_x}e_{\alpha_x}\\
&\quad + \Big(- \gamma_1\frac{m_s}{m}h\omega_z + \kappa_1\frac{b_x}{J_{x,s}}\mathcal{S}_{\omega_z}\\
&\qquad\qquad - p_{22}k_{o3} - p_{23}k_{o4}\Big)e_{v_x}e_{\omega_x}\\
&\quad - \frac{k_{x,e}}{J_{x,s}}e_{v_y}e_{\alpha_x} + \Big(\kappa_1\frac{m_s}{m}h|\omega_z| - \frac{b_x}{J_{x,s}}\Big)e_{v_y}e_{\omega_x}
\end{aligned}
$$

where

$$
P_2 = P_2^T = \begin{pmatrix} p_{21} & p_{22} \\ p_{22} & p_{23}\end{pmatrix} > 0
$$

has been determined as solution of the Lyapunov equation

$$
P_2 A_2 + A_2^T P_2 = -Q_2, \qquad Q_2 = Q_2^T > 0.
$$

This expression can be simplified choosing the observer gains $k_{o1}, \cdots, k_{o4}$ such that

$$
\begin{aligned}
\begin{pmatrix} k_{o1} \\ k_{o2}\end{pmatrix} &= \frac{1}{\gamma_1 - \kappa_1^2}\begin{pmatrix} \frac{1}{2}\kappa_1\omega_{z,\max} + \kappa_1\gamma_1|\omega_z| \\ \frac{1}{2}\kappa_1^2\omega_{z,\max}\mathcal{S}_{\omega_z} + \gamma_1^2\omega_z\end{pmatrix}\\
\begin{pmatrix} k_{o3} \\ k_{o4}\end{pmatrix} &= P_2^{-1}\begin{pmatrix} \kappa_1\frac{k_{x,e}}{J_{x,s}}\mathcal{S}_{\omega_z} \\ -\gamma_1\frac{m_s}{m}h\omega_z + \kappa_1\frac{b_x}{J_{x,s}}\mathcal{S}_{\omega_z}\end{pmatrix}
\end{aligned}
\tag{10}
$$

so obtaining

$$
\begin{aligned}
\dot{V}_o(t,e) &= -\frac{1}{2}\kappa_1\omega_{z,\max}e_{v_x}^2 - \kappa_1|\omega_z|e_{v_y}^2 - \left\| \begin{matrix} e_{\alpha_x} \\ e_{\omega_x}\end{matrix} \right\|_{Q_2}^2\\
&\quad - \frac{k_{x,e}}{J_{x,s}}e_{v_y}e_{\alpha_x} + \Big(\kappa_1\frac{m_s}{m}h|\omega_z| - \frac{b_x}{J_{x,s}}\Big)e_{v_y}e_{\omega_x}
\end{aligned}
$$

Choosing

$$
Q_2 = \begin{pmatrix} \lambda_1 & 0 \\ 0 & \lambda_2\end{pmatrix} \tag{11}
$$

$\lambda_1, \lambda_2 > 0$ one gets

$$\dot{V}_o(t,e) \leq -\frac{1}{2}\kappa_1\omega_{z,\max}e_{v_x}^2 - \kappa_1\omega_{z,\max}e_{v_y}^2 - \lambda_1 e_{\alpha_x}^2 - \lambda_2 e_{\omega_x}^2 + \frac{k_{x,e}}{J_{x,s}}e_{v_y}e_{\alpha_x} + \left(\kappa_1\frac{m_s}{m}h|\omega_z| - \frac{b_x}{J_{x,s}}\right)e_{v_y}e_{\omega_x}$$

where it has been considered that $|\omega_z| \leq \omega_{z,\max}$ (Assumption 1).

The cross terms can be eliminated using the following inequalities

$$\begin{aligned}\pm\alpha_1 e_{v_y}e_{\alpha_x} &\leq \frac{\alpha_1}{\mu_1}e_{v_y}^2 + \alpha_1\mu_1 e_{\alpha_x}^2\\ \pm\alpha_2 e_{v_y}e_{\omega_x} &\leq \frac{|\alpha_2|}{\mu_2}e_{v_y}^2 + |\alpha_2|\mu_2 e_{\omega_x}^2\\ &\leq \frac{\alpha_{2,\max}}{\mu_2}e_{v_y}^2 + \alpha_{2,\max}\mu_2 e_{\omega_x}^2\end{aligned}$$

thanks to Assumption 1, where $\mu_1, \mu_2 > 0$ are weighting terms, and

$$\alpha_1 = \frac{k_{x,e}}{J_{x,s}} > 0, \qquad \alpha_2 = \kappa_1\frac{m_s}{m}h|\omega_z| - \frac{b_x}{J_{x,s}}.$$

Hence,

$$\begin{aligned}\dot{V}_o(t,e) \leq &-\frac{1}{2}\kappa_1\omega_{z,\max}e_{v_x}^2\\ &-\left(\kappa_1\omega_{z,\max} - \frac{\alpha_1}{\mu_1} - \frac{\alpha_{2,\max}}{\mu_2}\right)e_{v_y}^2\\ &-\big(\lambda_1 - \alpha_1\mu_1\big)e_{\alpha_x}^2 - \big(\lambda_2 - \alpha_{2,\max}\mu_2\big)e_{\omega_x}^2.\end{aligned}$$

Setting

$$\begin{aligned}\kappa_1 &= \frac{1}{\omega_{z,\max}}\left(2\lambda_o + \frac{\alpha_1}{\mu_1} + \frac{\alpha_{2,\max}}{\mu_2}\right)\\ \lambda_1 &= \lambda_o + \alpha_1\mu_1\\ \lambda_2 &= \lambda_o + \alpha_{2,\max}\mu_2\end{aligned} \tag{12}$$

$\lambda_o > 0$, where $\mu_1, \mu_2 > 0$ can be chosen in order to ensure better performance, and κ_1 does not depend on time, one finally gets

$$\dot{V}_o(t,e) \leq -\lambda_o(e_{v_x}^2 + e_{v_y}^2 + e_{\alpha_x}^2 + e_{\omega_x}^2) < 0.$$

Hence, the error system in (9) has the origin exponentially stable, and the estimation errors (8) tend exponentially to zero, with a time constant $\tau = 1/\lambda_o$. We can conclude with the following.

Theorem 1. Under Assumption 1, when $|\omega_z| > 0$ the observer (7), with the gains (10), (12), ensures the global exponential convergence to zero of the estimation errors (8), with a time constant $\tau = 1/\lambda_o$, for a $\lambda_o > 0$ fixed by the designer. ◇

4. TYRE-ROAD FRICTION COEFFICIENT ESTIMATION

The interaction of a tyre with the ground is defined by a longitudinal force (F_x), a lateral force (F_y), a vertical force (F_z), and an aligning moment (M_z). The forces F_x, F_y, F_z and the moment M_z are applied to the wheels and reacted by the ground in the center of tyre contact (CTC). The effects of overturning moment (M_x), which are small for most maneuvers, are not included in this models.

The mass of the vehicle contributes the major portion of the total normal forces on the tyres. The lateral and longitudinal forces acting on the vehicle redistribute the normal forces between the tyres. Anyway, the instantaneous vertical tyre force can be calculated by knowing the instantaneous vertical compression of the tyre (σ_z) and its vertical spring rate C_z as the following:

$$F_z = \sigma_z C_z \tag{13}$$

where σ_z is defined as the spatial relationship between the wheel center (WC) and the center of tyre contact (CTC). On the other hand, the lateral and longitudinal tyre deflection (y_b, x_b) can be calculated by subtracting the lateral and longitudinal position of the (WC) to the lateral and longitudinal position of the (CTC) obtaining the same result given by an optical sensor as in (Tuononen *et al.*, 2008) (Tuononen *et al.*, 2008) (Tuononen, 2009) (Tuononen and Matilainen, 2009) (Tuononen, 2009) as shown in Fig. 2

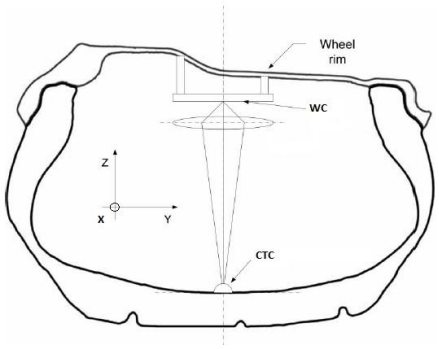

Fig. 2. Tyre Deflection.

The lateral deflection profile of the tyre's equatorial line, y_b is assumed to be a parabolic function of the contact patch position, x_b (Hong *et al.*, 2013) (Erdogan *et al.*, 2011):

$$y_b = \frac{F_y}{2C_{bend}}x_b^2 + \frac{F_y}{C_{lat}} \tag{14}$$

By applying the curve fitting technic to x_b, y_b in (14) one can find the estimation of the lateral force $\hat{F}_y$ for a given C_{bend}, C_{lat} coefficients representing the tyre bend and shift stiffness respectively.

This technique describes the tyre lateral deflection under the following assumptions:

1. The tyre deflection profile measured inside the contact patch is assumed to be a continuous function of the time.
2. During the driving maneuver, the tyre is in full adhesion condition.
3. The tyre is rigid for yaw dynamics and the aligning moment effects M_z can be neglected.

Therefore, the tyre-road friction coefficient is estimated through a tyre brush model in equations (15) which correlates the tyre-road friction coefficient $\hat{\mu}_y$, the estimated tyre slip angle $\hat{\alpha}_{11}$ and the sliding tyre slip angle α_{sl} with the estimated lateral force $\hat{F}_{y,11}$. The sliding tyre slip angle represents the limit tyre slip angle before the tyre starts

sliding. The friction coefficient $\hat{\mu}_y$ is estimated by solving the following nonlinear equations as in (Hong *et al.*, 2013) (Erdogan *et al.*, 2011)

$$\hat{F}_{y,11} = 3\hat{\mu}_y F_z \frac{\tan(\hat{\alpha}_{11})}{\tan(\alpha_{sl})}\Big(1 - \Big|\frac{\tan(\hat{\alpha}_{11})}{\tan(\alpha_{sl,11})}\Big| + \frac{1}{3}\frac{\tan^2(\hat{\alpha}_{11})}{\tan^2(\alpha_{sl})}\Big)$$
$$\hat{\mu}_y = \frac{2C_{py}a^2}{3F_z}\tan(\alpha_{sl}) \tag{15}$$

where: C_{py} is a given lateral stiffness of a tyre tread element, F_z is the normal force and a is the half length of the tyre-road contact patch calculated as in (Hong *et al.*, 2013):

$$a = \sqrt{2R(\Delta R) - (\Delta R)^2} \tag{16}$$

where R is the wheel radius and ΔR is the maximum value of the measured vertical tyre deflection.
Here:

$$\hat{\alpha}_{11} = \delta - \arctan\Big[\frac{\hat{v}_x\hat{\beta} + l_f\omega_z}{\hat{v}_x - E\omega_z/2}\Big] \tag{17}$$

with $\hat{\beta} = \hat{v}_x/\hat{v}_y$

5. SIMULATION RESULTS

In this section the behavior of the proposed nonlinear observer is shown for an interesting case, in which the vehicle performs a circular maneuver. The driver performs a constant steer of 23°. During the imposed maneuver, the tyre–road friction coefficient varies from $\mu_y = 0.9$ (dry surface) to $\mu_y = 0.5$ (wet surface) at $t = 4$ s and the tyre deflection is only measured into the front-left wheel with $R = 0.16$ m.

The initial longitudinal velocity is $v_x(0) = 28$ m/s (about 100 km/h) and the vehicle moves in a constant target speed. The initial values of the observer variables are

$$\hat{v}_x(0) = v_x, \quad \hat{v}_y(0) = 0, \quad \hat{\alpha}_x(0) = 0, \quad \hat{\omega}_x(0) = 0$$

and the nominal vehicle parameters, used in the observer (7), are given in Table 1.

Table 1.

Variable	Value	Unit	Variable	Value	Unit
m_0	1862	Kg	$b_{x,0}$	10000	$N\ m\ rad/s$
$m_{s,0}$	1592	Kg	$k_{x,0}$	114000	$N\ m/rad$
h_0	0.63	m	$J_{x,0}$	614	$Kg\ m^2$
$J_{z,0}$	2488	$Kg\ m^2$			

To show that the proposed observer is robust with respect to parameter variations, we have considered the parameters given in Table 2 for the vehicle dynamics (3).

Table 2.

Variable	Value	Unit	Variable	Value	Unit
m	1800	Kg	b_x	10000	$N\ m\ rad/s$
m_s	1550	Kg	k_x	114000	$N\ m/rad$
h	0.63	m	J_x	600	$Kg\ m^2$
J_z	2400	$Kg\ m^2$	l_f	1.18	m
l_r	1.77	m			

The obtained results are shown in Figure 3, with $k_{o1}, \cdots, k_{o4}$ in (7) set considering $\gamma_1 = 100$, $\kappa_1 = 9$ in (10), and $\lambda_1 = 1$, $\lambda_2 = 1000$ in (11). Notice the good tracking performance of the observer. Moreover, this nonlinear observer shows good performances with respect to system parameter variations. In particular, it is robust with respect variations of the tyre–road friction coefficient, since the performance does not depend relevantly on this crucial parameter. In Figure 4 the measured longitudinal and lateral accelerations, vertical tyre force and contact patch are presented. Notice that a random sensor noise has been considered. Finally in Figure 5 the estimation of the sideslip angle ($\hat{\beta}$), tyre slip angle ($\hat{\alpha}_{11}$), tyre lateral force ($\hat{F}_{y,11}$) and tyre-road friction coefficient ($\hat{\mu_y}$) are shown for $C_{lat} = 185$ kN/m, $C_{bend} = 10$ kNm, $C_{p,y} = 170$kN/m. Notice the good behavior of the estimations.

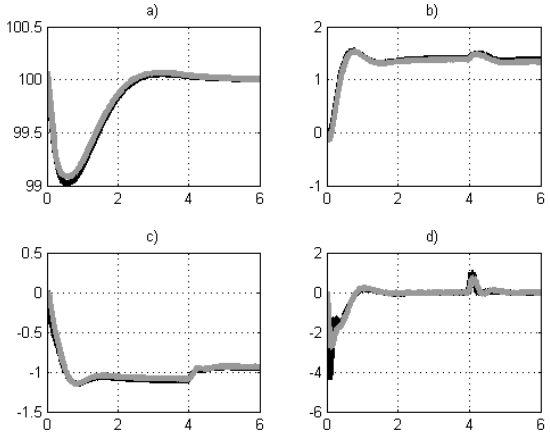

Fig. 3. a) Real longitudinal velocity v_x (black) and estimation $\hat{v}_x$ (gray) [km/h vs s]; b) real lateral velocity v_y (black) and estimation $\hat{v}_y$ (gray) [km/h vs s]; c) real roll position α_x (black) and estimation $\hat{\alpha}_x$ (gray) [deg vs s]; d) real roll rate w_x (black) and estimation $\hat{w}_x$ (gray) [deg/s vs s].

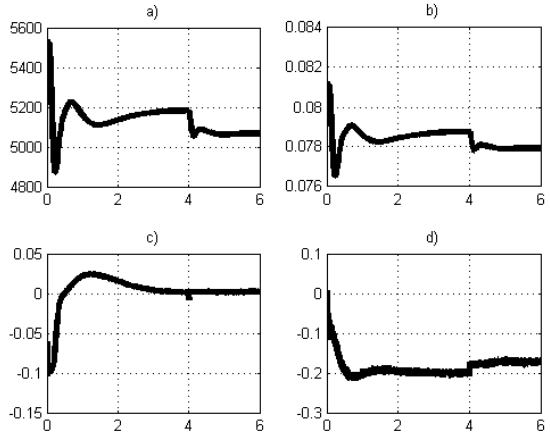

Fig. 4. a) Vertical tyre force $F_{z,11}$ [N vs s]; b) contact patch length a [m vs s]; c) measured longitudinal acceleration a_x [g's vs s]; d) measured lateral acceleration a_y [g's vs s].

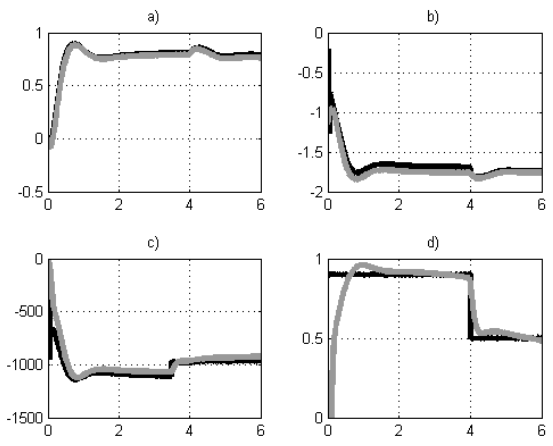

Fig. 5. a) Real sideslip angle β (black) and estimation $\hat{\beta}$ (gray) [deg vs s]; b) real tyre slip angle α_{11} (black) and estimation $\hat{\alpha}_{11}$ (gray) [deg vs s]; c) real tyre lateral force $F_{y,11}$ (black) and estimation $\hat{F}_{y,11}$ (gray) [N vs s]; d) real tyre-road friction coefficient μ_y (black) and estimation $\hat{\mu}_y$ (gray) [adimensional vs s].

6. CONCLUSION

This paper proposes a nonlinear observer for the lateral velocity and for the roll position and velocity. This observer uses the available measurements, as provided by the sensors usually present in a modern vehicle, i.e. the longitudinal and lateral accelerations, the longitudinal velocity, the yaw rate, and the steer angle. The observed variables are plugged into the brush model for tyre-road friction coefficient estimation based on tyre lateral deflection. Simulations show a good behavior of both observer and friction coefficient estimation.

REFERENCES

J. Farrelly, and P. Wellstead. Estimation of vehicle lateral velocity. *Proceedings of the 1996 IEEE International Conference on Control Applications*, pages 552–557, 1996.

Y. Fukada Slip-angle estimation for stability control. *Vehicle Systems Dynamics*, volume 32, pages 375–388, 1999.

H. Peng, A.Y. Urgonen, and H. Tseng. A study on lateral speed estimation methods. *International Journal on Vehicle Autonomous Systems*, volume 2, pages 126–144, 2004.

P. J. Venhovens, and K. Naab. Vehicle dynamic estimation using Kalman filters. *Vehicle Systems Dynamics*, volume 32, pages 171–184, 1999.

U. Kiencke, and A. Daiss. Observation of lateral vehicle dynamics. *Control Engineering Practice*, volume 5, no 8, pages 1145–1150, 1997.

U. Kiencke, and L. Nielsen. Automotive Control systems. *Springer*, Berlin, 2000.

M. Hiemer, A. VonVietinghoff, U. Kienke, and T. Matsunaga. Determination of vehicle body slip angle with nonlinear observer strategies. *Proceedings of the SAE World Congress*, no 2005-01-0400, 2005.

G. Baffet, J. Stephant, and A. Charara. Lateral vehicle-dynamic observers: simulations and experiments. *International Journal of Vehicle Autonomous Systems*, volume 5, no 3-4, pages 184–203, 2007.

J. Stephant, A. Charara, and D. Meizel. Evaluation of sliding mode observer for vehicle sideslip angle. *Control Engineering Practice*, volume 15, pages 803–812, 2007.

L. R. Ray Nonlinear state and tire force estimation for advanced vehicle control. *IEEE Transaction on Control Systems Technology*, volume 3, no 1, pages 117–124, 1995.

A. Suissa, Z. Zomotor and, F. Boettiger. Method for determining variable characterizing vehicle handling. *Patent US 5557520*, 1996.

M. C. Best, T. J. Gordon, and P. J. Dixon. An extended adaptative Kalman filter for real-time state estimation of vehicle handling dynamics. *International Journal of Vehicle Mechanics and Mobility*, volume 34, No 1, pages 57–75, 2000.

G. J. Heydinger, W. R. Garrott, J. P. Chrstos, and D. A. Guenther. A methodology for validating vehicle dynamics simulations. *Society of Automotive Engineers*, paper 900128, 1990.

M. Doumiati, A. C. Victorino, A. Charara, and D. Lechner. On-board real-time estimation of vehicle lateral tire-road forces and sideslip angle. *IEEE/ASME Transaction on Mechatronics*, volume 16, no 4, pages 601–614, 2011.

A. J. Tuononen Optical position to measure tyre carcass deflectioin. *Vehicle System Dynamics*, volume 46, no 6, pages 471–481, 2008.

A. J. Tuononen, and L. Hartikainen. Optical position detection to measure tyre carcass deflection in aquaplaning. *International Journal of Vehicle System Modelling and Testing*, volume 3, no 3, pages 189–197, 2008.

A. J. Tuononen On-board estimation of dinamic tyre forces from optical measured tyre carcass deflection. *Journal of Heavy Vehicle Systems*, volume 16, no 3, pages 362–378, 2009.

A. J. Tuononen, and M. J. Matilainen. Real time estimation of aquaplaning with an optical tyre sensor. *Journal of Automobile Engineering*, volume 223, no D10, pages 1263–1272, 2009.

A. J. Tuononen Vehicle lateral state estimation based on measured tyre forces. *Sensors*, volume 9, no 11, pages 8761–8775, 2009.

H. B. Pacejka Tyre and vehicle dynamics. *Elsevier Butterworth*, 2005.

S. Mammar, V. B. Baghdassarian, and L. Nouveliere. Speed scheduled vehicle lateral control. *International Conference on Intelligent Transportation Systems*, pages 80-85, 1999. Pacejka 2005

S. Hong, G. Erdogan, K. Hedrick, and F. Borrelli. Tyre road friction coefficient estimation based on tyre sensors and lateral tyre deflection: simulations and experiments. *Vehicle System Dynamics: International Journal of Vehicle Mechanics and Mobility*, volume 51, no 5, pages 627–647, 2013.

G. Erdogan, L. Alexander, and R. Rajamani. Estimation of tyre-road friction coefficient using a novel wireless piezoelectric tire sensors. *IEEE Sensors Journal*, volume 11, no 2, pages 267–279, 2011.